J|A|C|S COMMUNICATIONS

Published on Web 04/28/2010

# The Big Red Shift of Photoluminescence of Mn Dopants in Strained CdS: A Case Study of Mn-Doped MnS−CdS Heteronanostructures

Taisen Zuo,[†,§] Zhipeng Sun,[†,§] Yuliang Zhao,[†] Xiaoming Jiang,[‡] and Xueyun Gao*[,†]

*Lab for Biomedical Effects of Nanomaterials and Nanosafety and Beijing Synchrotron Radiation Laboratory, Institute of High Energy Physics, Chinese Academy of Sciences, Beijing 100049, P. R. China*

Received January 8, 2010; E-mail: gaoxy@ihep.ac.cn

Transition-metal-doped nanosemiconductors have attracted more attention in the past few years because of their interesting optical properties.[1−5] For example, the d electronic states of Mn ions act as luminescent centers while interacting strongly with the s and p electronic states of the host nanocrystal into which external electronic excitation is directed, and an orange photoluminescence is produced therein.[3−5] However, when Mn-doped nanocrystals are utilized in bioimaging, longer-wavelength emissions are more desirable.[6] To date, no approaches for achieving the red emission of Mn dopants in situ have been reported, although their emission could shift to lower energies when gigapascal-level hydrostatic pressure is applied to them in a diamond anvil cell because the external high pressure makes the crystal-field splitting of the Mn d orbitals become narrower.[7] To overcome the disadvantage of hydrostatic pressure via a diamond anvil cell, we explored a new way to introduce lattice strain to Mn dopants in host nanocrystal via heteronanostructure growth, where Mn-doped CdS nanocrystals crystallize onto the surface of MnS nanoparticles. Because of the difference between the lattices of MnS and CdS, in situ lattice compression of CdS occurs. Such compressions result in lattice strain in CdS, as would occur with external hydrostatic pressure, and further change the emission of Mn dopants to a longer wavelength. In our studies, such an approach was able to change the emission of Mn dopants from orange to red, meaning that gigapascal-level stress occurred in Mn dopants in MnS−CdS heteronanostructures in situ.[7]

The Mn-doped MnS−CdS heteronanostructures, pristine MnS and CdS nanoparticles, and Mn-doped CdS were synthesized via facile metal−organic reactions (see section S1 in the Supporting Information). In order to observe the lattice compression of CdS in MnS−CdS heteronanostructures, high-resolution transmission electron microscopy (HRTEM) was used to study the lattice fringes of MnS−CdS, MnS, and CdS nanoparticles (see section S2). Figure 1a shows the pristine MnS nanoparticles; the upper-left inset shows nanoparticles with diameters of 2−3 nm. Fast Fourier transform (FFT) analysis was conducted on a selected area of a single nanoparticle in Figure 1a, and the results are displayed in the upper-right inset. The FFT clearly showed that the *d* spacings of (110) and (002) are 0.200 and 0.323 nm, respectively, which are in good agreement with those of hexagonal MnS with the wurtzite structure (see JCPDS card no. 41-1049). HRTEM images and FFT data of single Mn-doped MnS−CdS heteronanostructures are displayed in Figure 1b. FFTs of selected areas located in the lower and upper parts of the MnS−CdS image are displayed in upper-left and upper-right insets, respectively. In the lower part of the MnS−CdS image, the *d* spacings of (100) and (002) are 0.352 and 0.325 nm, respectively, which match those of hexagonal MnS with the wurtzite

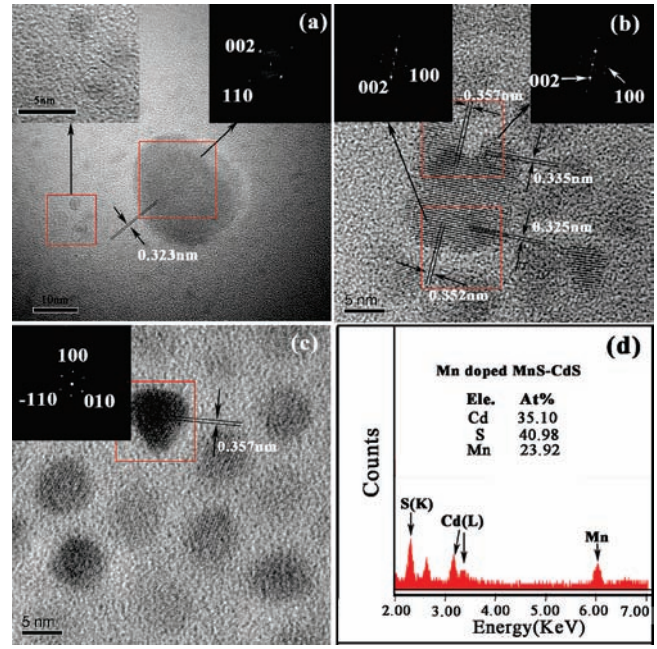


***Figure 1.*** (a−c) HRTEM images and (insets) FFT patterns of (a) pristine MnS, (b) Mn-doped MnS−CdS, and (c) pristine CdS. (d) EDS data for Mn-doped MnS−CdS.

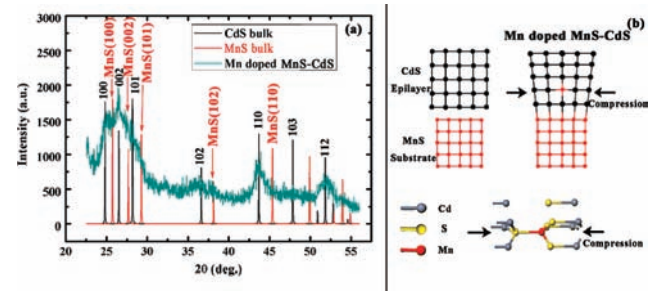


***Figure 2.*** (a) XRD patterns of Mn-doped MnS−CdS. (b) Illustrations of the compression of the *d* spacing of CdS at the MnS−CdS interface.

structure (see JCPDS card no. 41-1049). Notably, the *d* spacing of 0.325 nm for this (002) is similar to the value of 0.323 nm for pristine MnS in Figure 1a. In the upper part of the MnS−CdS image, the *d* spacings of (100) and (002) are 0.357 and 0.335 nm, respectively, which match those of hexagonal CdS with the wurtzite structure (see JCPDS card no. 65-3413), and the (100) *d* spacing of 0.357 nm is the same as that of pristine CdS displayed in Figure 1c. HRTEM observations of single MnS−CdS nanocrystals showed no defects in the lattice fringes in MnS−CdS heteronanostructures although there is a lattice mismatch between bulk CdS and MnS, implying that the larger *d* spacing of CdS was compressed to match

[†] Lab for Biomedical Effects of Nanomaterials and Nanosafety.
[‡] Beijing Synchrotron Radiation Laboratory.
[§] These authors contributed equally.



**10.1021/ja100136a** 

the smaller spacing of MnS in the interfaces of MnS−CdS.[7] The energy-dispersive spectroscopy (EDS) data for MnS−CdS heteronanostructures in Figure 1d clearly disclosed the Cd, Mn, and S components in the MnS−CdS heteronanostructures.

It is known that bulk wurtzite MnS has a smaller *d* spacing than wurtzite CdS. In our MnS−CdS growth, the *d* spacing of CdS should shrink to match that of MnS, and Mn ions could diffuse into CdS at the MnS−CdS interface to form Mn-doped CdS, where Mn ions replace some Cd ions in CdS matrix.[1,2,7] To further confirm the MnS−CdS heteronanostructures, powders of MnS−CdS were studied by X-ray diffraction (XRD; see section S3). The XRD patterns in Figure 2a showed that wurtzite-structured MnS and CdS are both present in the MnS−CdS heteronanostructures. In detail, peaks of hexagonal CdS can be distinctly observed, and peaks of hexagonal MnS at 25.4° {100}, 27.5° {002}, 29.05° {101}, 37.78° {102}, and 44.78° {110} are also visible in the MnS−CdS samples; these results are consistent with the HRTEM studies in Figure 1b. The *d* spacings of MnS and CdS derived from the XRD patterns are shown in Table 1. Obviously, these *d* spacings of MnS and CdS are similar to those of bulk hexagonal MnS and CdS, respectively (see JCPDS card nos. 41-1049 and 65-3413). Because no defects were detected within the MnS−CdS heteronanostructures in the HRTEM observations in Figure 1b, we believe that the compression of CdS occurs mainly at the MnS−CdS interface, where the Mn dopants are more concentrated in the CdS matrix.[1,2] According the XRD data in Figure 2a and Table 1 as well as the HRTEM studies in Figure 1, an illustration of the Mn-doped MnS−CdS heteronanostructure is disclosed in Figure 2b. It is clear that the *d* spacing of CdS is compressed to match that of MnS at the interface; such shrinking of CdS introduces lattice strain and further suppresses the Mn−S bond in the Mn-doped CdS matrix.[7,8] Consequently, the crystal-field splitting of the 3d orbitals ($^4T_1 \rightarrow {}^6A_1$ transition) became narrower, resulting in a red shift of the Mn ion emission.[8]

***Table 1.*** Interplanar Distances of MnS and CdS in MnS−CdS Heteronanostructures

| plane | MnS in MnS−CdS | CdS in MnS−CdS |
|---|---|---|
| 100 | 3.504 | 3.553 |
| 002 | 3.241 | 3.367 |
| 101 | 3.070 | 3.187 |
| 102 | 2.380 | 2.469 |
| 110 | 2.022 | 2.068 |
| 112 | − | 1.761 |

The optical absorption and emission of Mn-doped MnS−CdS and Mn-doped CdS are shown in Figure 3a (see section S4). The absorption peaks of Mn-doped MnS−CdS and Mn-doped CdS are located at ~458 and 449 nm, respectively, which corresponds to a size-dependent CdS transition. The normal emission of Mn-doped CdS is at ~585 nm, which is very close to the wavelength reported for Mn ion emission in doped II−VI semiconductors.[3−5] However, such emission peaks disappear in Mn-doped MnS−CdS because the electronic excitation of the CdS matrix is directed into the 3d electrons of the Mn dopants under exposure to lattice strain. Consequently, the stress-narrowed $^4T_1 \rightarrow {}^6A_1$ transition of Mn ions produced the red emission at 650 nm. To our knowledge, all previously reported emissions of Mn dopants in II−VI nanosemiconductors are located at ~585 nm when these materials are under normal pressure.[3−5] The lattice strain in MnS−CdS induced a big shift in the Mn emission from orange to red, which implies that gigapascal-level stress occurred in the CdS matrix.[8] The photoluminescence (PL) decay times of Mn dopants in CdS and MnS−CdS matrix are displayed in Figure 3b (see section S4). The

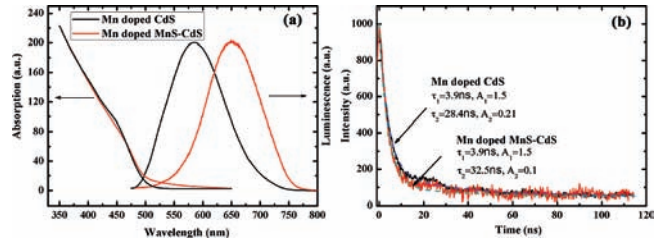


***Figure 3.*** (a) UV−vis and PL spectra of Mn-doped CdS and Mn-doped MnS−CdS. (b) PL decay spectra of Mn-doped CdS and Mn-doped CdS upon excitation by a 355 nm laser.

decay curves were fitted with double-exponential functions according to the following formula:

$$Y = A_1 \exp(-t/t_1) + A_2 \exp(-t/t_2) + B$$

where $Y$ is the PL intensity and $B$ is the baseline intensity of the PL curve. For Mn in MnS−CdS, the corresponding coefficients $A_1$ and $A_2$ were 1.53 and 0.1, and the decay times $t_1$ and $t_2$ were 3.9 and 32.5 ns, respectively. For Mn in CdS, $A_1$ and $A_2$ were 1.5 and 0.21, and the decay times $t_1$ and $t_2$ were 3.9 and 28.4 ns, respectively. Obviously, Mn ions in CdS and MnS−CdS have similar PL decay characteristics, and these data match the fast decay time previously reported for the $^4T_1 \rightarrow {}^6A_1$ transition of Mn.[5,9] Recently, Godlewski and co-workers[9] proposed a model of spin-flip interactions between $Mn^{2+}$ and free carriers that could well explain the nanosecond decay times of our samples.

In conclusion, the red emission of $Mn^{2+}$ dopants in MnS−CdS heteronanostructures has been observed for the first time. Obviously, such emission of Mn resulted from the lattice stress raised in heterogrown MnS−CdS in situ and not from external hydrostatic pressure. In detail, the lattice spacings of CdS are compressed to match those of MnS at the MnS−CdS interface, and the compressed CdS matrix further makes the crystal-field splitting of the Mn 3d orbitals smaller. In addition, because Mn-doped MnS−CdS heteronanostructures combine the paramagnetism of MnS and the red emission of Mn dopants, such nanostructures may have more advantages either for magnetic resonance imaging or fluorescence imaging.[10]

**Acknowledgment.** We are thankful for the funding support from the NSFC (30870677), the 973 Program (2007CB935604, 2006CB705601, 2009CB930204), and the CAS Knowledge Innovation Program.

**Supporting Information Available:** Preparation of MnS, CdS, Mn-doped CdS, and Mn-doped MnS−CdS nanocrystals and TEM, XRD, and optical characterizations of these samples. This material is available free of charge via the Internet at http://pubs.acs.org.

## References

(1) Norris, D. J.; Efros, A. L.; Erwin, S. C. *Science* **2008**, *319*, 1776.
(2) Erwin, S. C.; Zu, L.; Haftel, M. I.; Efros, A. L.; Kennedy, T. A.; Norris, D. J. *Nature* **2005**, *436*, 91.
(3) Yang, Y.; Chen, O.; Angerhofer, A.; Cao, Y. C. *J. Am. Chem. Soc.* **2006**, *128*, 12428.
(4) Pradhan, N.; Goorskey, D.; Thessing, J.; Peng, X. *J. Am. Chem. Soc.* **2005**, *127*, 17586.
(5) Bhargava, R. N.; Gallagher, D. *Phys. Rev. Lett.* **1994**, *72*, 416.
(6) Gao, X.; Cui, Y.; Levenson, R. M.; Chung, L.W. K.; Nie, S. *Nat. Biotechnol.* **2004**, *22*, 969.
(7) Smith, A. M.; Mohs, A. M.; Nie, S. *Nat. Nanotechnol.* **2009**, *4*, 56.
(8) Li, G. H.; Su, F. H.; Ma, B. S.; Ding, K.; Xu, S. J.; Chen, W. *Phys. Status Solidi B* **2004**, *241*, 3248–3256.
(9) Godlewski, M.; Yatsunenko, S.; Ivanov, V. Yu.; Drozdowicz-Tomsia, K.; Goldys, E. M.; Phillips, M. R.; Klar, P. J.; Heimbrodt, W. *Low Temp. Phys.* **2007**, *33*, 192.
(10) Weissleder, R.; Pittet, M. J. *Nature* **2008**, *452*, 580.

JA100136A